Noninvasive Input Function Acquisition and Simultaneous Estimations With Physiological Parameters for PET Quantification: A Brief Review

David Dagan Feng, *Fellow, IEEE*, Kewei Chen, and Lingfeng Wen, *Member, IEEE*

***Abstract*—The recent introduction of high-resolution and high-speed PET/CT is making noninvasive absolute quantification of physiological function more convenient and feasible. A key issue for absolute quantification is the accurate estimation of the time-activity curve (TAC) in plasma (PTAC). We provide a brief survey of the population-based and the image-derived PTAC approaches together with their performance characterizations. We then give a summary of the recent report on the image-derived PTAC from the first total-body PET/CT device, uEXPLORER. We finally summarize the kinetic model-based simultaneous estimation of input functions and physiological parameters (SIME) method. SIME has several advantages, including the more adequately estimated local input function for adjacent tissue TACs; simultaneous correction of spillover and partial-volume effect; smoothing the measurement noise and alleviating the need for the measurement of the PTAC peak; and simultaneous estimation of multiple input functions for organs such as the liver where blood is supplied from the hepatic artery and the portal vein. As the SIME approach is intended to improve the quality of quantification, it is expected that the image-derived PTAC from the total-body PET scanner together with the SIME approach will advance future PET absolute quantitative studies.**

***Index Terms*—Biological system modeling, image processing, molecular imaging, parameter estimation, positron emission tomography (PET).**

I. Introduction

THE DEVELOPMENT of positron emission tomography/computed tomography (PET/CT) scanners with much improved temporal and spatial resolution, greater sensitivity and a larger axial field of view (FOV) now offers the potential to obtain absolute quantification of physiological parameters simultaneously from multiple tissues/organs in the entire body. Different from the visual, qualitative or semiquantitative assessments, the PET tracer kinetic modeling technique enables detailed and absolute quantification of physiological and biochemical processes in human and in animal studies *in vivo*. Measurements of the tracer time-activity curves (TACs) in plasma (PTAC) and tissue (TTAC) are required to estimate physiological parameters, i.e., to estimate the parameters of certain compartmental models by using PTAC as the input and the TTAC as the model output function. Previously, PTAC was obtained by taking blood samples invasively from an artery or arterialized vein [1]–[3]. It is obvious that the insertion of arterial lines and the subsequent collection and processing of arterial blood is not compatible with the practice of clinical PET, as it requires extra personnel and processing time, exposes the patient to the risks associated with the insertion of an arterial line, and exposes personnel to the risks associated with the handling of patient blood and increased radiation from proximity to the patient [4]. Therefore, it is of interest to develop practical noninvasive techniques for tracer kinetic modeling with PET. Such interest has been especially highlighted for clinical research and in brain imaging for the past years [5]. A recent review paper covered various areas related to PET quantifications in the concepts of parametric imaging, kinetic models and parameter estimation methods, and challenges and associated correction methods [6]. Some noninvasive techniques have been reviewed in an abstract context in this review paper. Among these, for example, the parameters can be directly estimated from sinogram in reconstruction [7], [8]. In this article, we will provide a brief review of noninvasive input function acquisition and simultaneous estimations with physiological parameters, including summarizing our previous representative works in this area. We will use primarily fluorodeoxyglucose (FDG)-PET as a practical example for various ways to acquire and estimate PTAC. Applications for other PET tracers will be mentioned too.

Manuscript received April 18, 2020; revised June 21, 2020; accepted July 5, 2020. Date of publication July 21, 2020; date of current version November 3, 2020. *(Corresponding author: David Dagan Feng.)*

David Dagan Feng is with the Biomedical and Multimedia Information Technology Research Group, School of Computer Science, University of Sydney, NSW 2006, Australia, and also with the School of Biomedical Engineering, Shanghai Jiao Tong University, Shanghai 200240, China (e-mail: dagan.feng@sydney.edu.au).

Kewei Chen is with Banner Alzheimer's Institute, Phoenix, Arizona, AZ 85006 USA (e-mail: kewei.chen@bannerhealth.com).

Lingfeng Wen is with the Department of Molecular Imaging, Royal Prince Alfred Hospital, Camperdown, NSW 2050, Australia, and also with the Biomedical and Multimedia Information Technology Research Group, School of Computer Science, University of Sydney, NSW 2006, Australia (e-mail: wenf@ieee.org).

Color versions of one or more of the figures in this article are available online at http://ieeexplore.ieee.org.

Digital Object Identifier 10.1109/TRPMS.2020.3010844

II. Two Commonly Used Approaches Toward Noninvasive Input Function Acquisition

Tremendous effort has been made to reduce or eliminate invasive blood sampling in PET quantification. The blind estimation approach can eliminate the necessity of measuring the input function when performing dynamic studies under certain conditions, such as quantification of cerebral blood flow that

do not require a blood fraction term are amenable to the blind estimation approach [9]. Most of the other approaches focused on reducing the number of blood samples or acquiring blood samples noninvasively. For example, the minimum number of arterial blood samples was investigated for the quantification of cerebral metabolism for glucose (CMRglu) [10]. A biexponential modeling of the input function to fit the reduced number of blood sampling was introduced in the early 1980s [11]. The method used by Kato *et al.* was not aimed to precisely capture the full dynamics of the input function. Instead, they examined the accuracy of the CMRglu, with an estimated input function (EIF) that missed the initial peak. They first generated a dummy input function by extrapolating the blood data points after 2 min back to 0 min (with a bolus injection of the tracer, the peak appeared within the first 2 min). They then fitted the reduced number of blood samples by a biexponential curve as the input function. They claimed that the error introduced into the CMRglu by using these different approximations was <3%. This approach has a distinctive advantage that it only requires a small number of blood samples. However, it compromises the accurate estimate of the input function, and is not capable of accounting for the variation of tracer injection duration and time, and it may not provide the required accuracy where the estimations of individual microparameters are needed.

A. Population-Based Approaches

The population-based approach was introduced to reduce, or to minimize, but not to completely eliminate, the blood sampling for each individual study participant or patient. In 1993, the population-based approach was reported to estimate the input functions from a population-based arterial blood curve for FDG-PET studies with bolus injections [12]. Such a method was used to deal with the challenges related to the very fast dynamic acquisition right after the tracer injection. During that time, PET scanners were not able to acquire the fast kinetics of the physiological event. Note that such an issue did not exist for TTAC due to the slowness of its dynamics. With a total of 34 subjects, the population-based blood curve was generated based on the first 10 and evaluated in the remaining 24 subjects. An EIF was obtained by scaling the population-based curve with two arterial blood samples, one obtained at 10 min and the other at 45 min. The authors found that the time integrals for EIF and the real arterial input function (RIF) were in excellent agreement ($r = 0.998, P < 0.0001$). More importantly, CMRglu calculated with EIF, RIF, and the autoradiographic technique, which is an invasive imaging technique, and which can only acquire a static imaging with the use of mean rate constants of the compartmental model for gray matter [3], also correlated strongly ($r = 0.992, P < 0.0001$). Their results suggested that individually scaled, population-derived input functions may serve as an adequate alternative to continuous arterial blood sampling in quantitative FDG-PET imaging. The autoradiographic method [3] was widely used to derive CMRglu images in clinical neurologic studies because of shorter scanning times and the requirement for fewer blood samples, such as with two arterialized venous samples at 10 and 45 min [13], one arterial sample at 12 min [14], or one nonarterialized venous sample at 40 min [15], to scale the population-based input function. The population-based method with scaled blood samples has been also extended to other PET tracers, such as in the assessment of skeletal kinetics using ^{18}F-fluoride [16], bone perfusion and metabolism using ^{18}F-NaF [17], and neuroreceptor study using 2-^{18}F-fluoro-A-85380 [18] and ^{11}C-(R)-rolipram [19].

The major weaknesses of the population-based approaches are: 1) it is not completely noninvasive and a smaller number of blood samples is still needed to tailor the population-based curve to an individual subject. Therefore, it may be more appropriate to be classified into the minimal invasive approach and 2) the accuracy of the physiological parameter estimation is highly dependent on the accuracy of the population-based input function, but it is not flexible enough to meet the variations of each individual input function based on fitting a couple of purposely collected blood samples. In other words, the population-based curve is fixed in shape which can only be scaled by 1 or 2 blood samples, and hence may not meet the required accuracy to substitute the true PTAC.

B. Image-Derived Methods

The idea of using an image-derived input function (IDIF) in place of blood sampling has been extensively studied from a very early days of PET tracer kinetic modeling. As introduced in [12], dynamic acquisition of radioactivity from the cardiac blood pool [20]–[25], the descending aorta [26], the abdominal aorta [27]–[29], the carotid artery [4], [30], and the radial artery [31] has been employed to acquire usable noninvasive input functions. The basic idea of the IDIF is straightforward. From the data acquisition perspective, the only requirement, different from acquiring TTAC, is the fast frame rate in the first 1.5 to 2 min to capture the peak of the input function from the bolus injection. From our own study published in 1998 [4], we managed to get the PET scanner and the associated computer system (Siemens, Knoxville, TN, USA) configured such that the images with frame duration as short as 2 s were acquired. Acquisition started at the time of the tracer injection and lasted for a total of 60 min. The acquisition protocol was as follows: one frame of 12 s (allowing the delivery of the tracer to the carotid artery), eight frames of 2 s each, two frames of 10 s each, one 12-s frame, one 30-s frame, two 60-s frames, two 90-s frames, one 3.5-min frame, two frames of 5 min, one frame of 10 min, and one frame of 30 min. PET images were acquired from 12 to 48 s were summed and used to identify the carotid artery to eliminate the need for acquiring magnetic resonance (MR) imaging data and subsequent co-registration with PET. To account for the partial-volume effect due to the small size of the carotid artery, we also did arterialized venous blood sampling at three time points toward the end of the scan.

At any time t, the measurement C_p^{mea} from the carotid artery region of interest (ROI) was assumed to be a linear combination of two components: 1) the (true) radioactivity from the blood vessel and 2) the radioactivity from the surrounding tissues as shown in

$$C_p^{mea}(t) = rc \times C_p(t) + m_{tb} \times C_t(t) \quad (1)$$

where C_p was the true (spillover free) radioactivity in the blood pool and C_t was the radioactivity from the surrounding tissue; rc was the recovery coefficient, and m_{tb} was the spillover coefficient from the tissue to the blood vessel. Both rc and m_{tb} were time independent, non-negative constants less than 1. However, similar to the situation in which the spillover from tissue to blood pool is solely from surrounding tissue, as in [20], the constraint $rc+m_{tb} = 1$ was not put onto these two parameters. In this study, C_p^{mea} was the dynamic data obtained from the carotid artery ROI on the PET images, C_t was acquired over the tissue ROI. The measurement of C_p was approximated by the venous blood samplings after the radioactive concentration had been equilibrated between the arterial and venous vessels. Based on (1) at the time points where the measurements for all three TACs were available, the linear least-square method could then be used to estimate rc and m_{tb}. When the estimates of rc or m_{tb} from the linear least square method were less than 0 or greater than 1, the non-negative linear least-square technique was applied to obtain new estimates that were guaranteed to be non-negative. The input function generated using this approach can capture the full dynamic as the blood sample-based input function. We have also validated the accuracy of this noninvasive approach with the regular invasive blood sampling approach. Taking advantage of widely available MR scanners, the use of MR scans to capture the carotid artery has been investigated [32], [33]. MR images also offer the opportunity to more adequately account for the spillover and partial-volume effect using more advanced correction techniques.

Various approaches have been presented to correct partial volume and spillover for the image-derived input function in brain studies [34]–[37]. Efforts have also been made to combine image processing to objectively delineate the ROIs for image-based noninvasive input functions. For example, the profile fitting method was presented to derive aorta-based input function [38], while cluster analysis was applied to group similar TTACs to identify ROIs for use in deriving the input functions [39]–[41]. Similarly, the independent component analysis (ICA) method was also used in the noninvasive analysis of dynamic images [41]–[44].

The main advantage of the IDIF is that it is almost completely noninvasive. However, the disadvantages include: 1) a limited FOV in the regular scanners and hence TTAC and PTAC may have to be obtained from different FOVs at different times; 2) full (and therefore long) dynamic imaging required right after the injection of tracer; 3) experience-dependent and subjective human errors in handling the spillover, partial volume, metabolites, and decay corrections for PTAC; and 4) the actual PTAC derived from TTACs (from images), e.g., in brain study, may be slightly different from the image-derived PTAC from a remote area where large blood pools can be seen more obviously, e.g., in the left ventricle (LV) or aorta, while spillover and partial volume contamination is too strong in the carotid artery. The image-derived PTAC would be still applicable for tracers with metabolites when a population-based metabolite correction profile is available, stable and validated for use among different subjects [6]. It is also worth noting that the metabolites in the blood for many tracers which are widely utilized clinically are not an issue or ignorable.

With total-body PET scanners, such as with the uEXPLORER and PennPET EXPLORER, it becomes feasible to obtain simultaneous dynamic imaging for the entire human body, from head to toes. Such a scanner enables the input functions to be extracted from the multiple blood structures and has overcome most of the issues for IDIF mentioned above [45]. Using the uEXPLORER, Zhang *et al.* [46] extracted PTACs, via the IDIF approach, from five blood regions—LV, aorta, carotid artery, brachial artery, and femoral artery, and obtained TTACs for four major organs/tissues—myocardium, liver, the gray matter and white matter of the brain simultaneously. The comparison of the results demonstrated the subtle differences among the five PTACs, providing an insightful understanding of the behaviors of these different PTACs. They also found that the arterial curves measured from the carotid, brachial, and femoral arteries resulted in lower peaks than the peak of the aorta due to the dispersion and partial-volume effects. In their paper, they suggested that, by taking into account of the motion and partial-volume effects, the aorta blood structure was the most ideal structure for use in parametric imaging. The data in [46] provide a base to compare the advantages and disadvantages of IDIF from the cardiac blood pool, the descending aorta, the abdominal aorta, the carotid artery, and the radial artery.

III. PTAC Model-Based Input Function

While the total-body PET scanner can provide the direct measurement of image-derived PTAC from various parts of the body where the blood pool can be identified, the model-based PTAC approach reviewed in detail in this section will provide added advantages for the estimation of the input function through modeling on top of the directly measured PTAC and TTAC, or TTAC alone. For example, this modeling would get a more accurate and uncontaminated PTAC (e.g., by removing measurement noise, spillover, and partial-volume effects), or hardly directly measurable PTAC (e.g., the intracerebral arteries from brain images or portal vein (PV) from liver images), that directly drives the measured TTAC, as well as to improve the physiological parameter estimation accuracy and to possibly get additional useful physiological parameters, such as α_v, the relative portal venous contribution to the hepatic blood flow, which may provide an important, additional and alternative indicator for liver cancer detection. As the PTAC model-based simultaneous estimation approach is intended to improve the quality of quantification, it is expected that the image-derived PTAC from the total-body PET scanner together with the PTAC model-based simultaneous estimation approach will advance future PET absolute quantitative studies.

The population-based and IDIF approaches are designed to estimate the PTAC first, which is then used to estimate physiological parameter with dynamic PET data. However, it is possible to estimate PTAC simultaneously together with the physiological parameters based on multiple TTACs from different parts of images only, as PTAC is imbedded in these

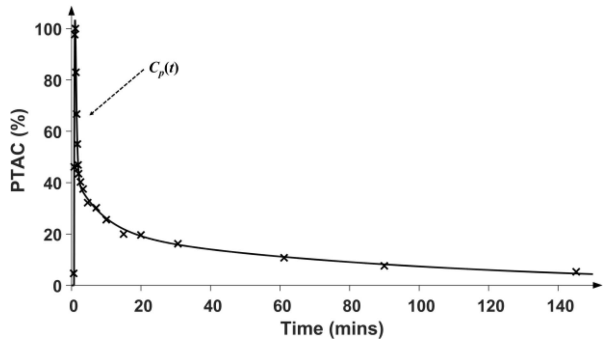

Fig. 1. Curve plot of fitted PTAC and "x" represents the measured samples from the arterialized vein at 0.63, 0.79, 0.94, 1.13, 1.31, 1.49, 1.69, 1.87, 2.04, 2.60, 3.33, 4.64, 7.13, 10.03, 15, 20, 30.61, 61.15, 90, and 145.18 min.

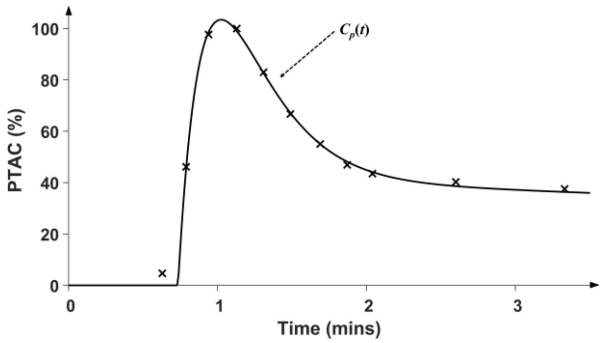

Fig. 2. Curve plot for the fitted PTAC for the first 3 min. "x" represents the measured samples from the arterialized vein at 0.63, 0.79, 0.94, 1.13, 1.31, 1.49, 1.69, 1.87, 2.04, 2.60, and 3.33 min.

images. In other words, any TTAC seen in one location of the image is driven by PTAC with the underlying physiological, biochemical and biological processes described by a kinetic model, such as the FDG model. If there is an appropriate model or analytical expression for PTAC, then the parameters of this PTAC model or analytical expression, will likely be estimated together with the parameters corresponding to the kinetic model. As the PTAC has also to follow some kind of combination of flow kinetics, diffusion and metabolic kinetics, it can thus be described, or at least be approximated, by another kinetic model and eventually by an explicit analytic expression. In our prior work [47], we discovered that, using FDG experimental data, it was possible to develop a generic model or an analytical expression for PTAC kinetics.

Based on the conceptual 4-compartment model proposed in [47], an analytical solution with mathematical expression of PTAC has been derived. However, there may be, of course, many other possible mathematical alternatives. In [47], five possible candidates (mathematical expressions of PTAC) were short listed. In order to validate the PTAC model, system identification, model discrimination, and various statistical criteria were used to evaluate this model with other possible model candidates. A fourth-order exponential equation with a pair of repeated eigenvalues in (2) is proven to be the most suitable model to describe the kinetics of PTAC

$$\begin{aligned} y(t) &= [A_1(t-\tau) - A_2 - A_3]e^{\lambda_1(t-\tau)} + A_2 e^{\lambda_2(t-\tau)} \\ &\quad + A_3 e^{\lambda_3(t-\tau)}, \quad \text{if } t \geq \tau \\ &= 0, \quad \text{if } t < \tau \end{aligned} \tag{2}$$

where λ_1, λ_2, and λ_3 are the eigenvalues of the model; A_1, A_2, and A_3 are the coefficient constants; and τ is the time-delay constant. For convenience, the model described by (2) is often referred to as the PTAC model, Feng's AIF model, or Feng's IF model in some literature.

Fig. 1 plots the fitted PTAC based on (2) with the samples from a clinical data set in [47].

The PTAC model-based input function addresses the issue of PTAC peak which may not be described by the population-based approach or be observed by the IDIF method. One advantage of the PTAC model-based method is capable of estimating the peak time t_{peak} by fitting the curve with the samples when the first derivative of $y(t) = 0$. Fig. 2 plots the aforementioned PTAC curve for the first 3 min for better visualization.

The PTAC model was used to improve the estimation of the local CMRglu for FDG human studies in [47] and also applied to investigate the effect of measurement noise in PTAC [48] on the reliability of the estimation of CMRglu with computer simulation. This PTAC model has also been used in the software package PMOD (PMOD Technologies Ltd., Zürich, Switzerland) as in the PKIN tool (General kinetic modeling tool), for fitting blood TAC or PTAC, as well as in COMKAT (Compartment Model Kinetic Analysis Tool). In [49], the optimal sampling schedule of PTAC was suggested to be with six sampling points (or seven sampling points if the time-delay constant τ was included). Similarly, if image-based input function is available, six dynamic PET images would be sufficiently enough for accurate estimation of the six parameters required for the PTAC model (λ_1, λ_2, λ_3 and A_1, A_2, A_3), or seven dynamic PET images would be required to additionally include the extra parameter τ in the PTAC model. The optimal scanning schedule for the FDG study was also obtained using similar principles described in [50] and [51].

IV. Simultaneous Estimation of Input Functions and Physiological Parameters

A. PTAC-Based Parallel Modeling Approach—A Case Study for Cardiac Studies

In cardiac studies, the input function is often directly measurable from the cardiac images. However, due to the bidirectional spillover between the LV blood pool and myocardium wall, the measured tracer concentrations in LV blood pool $C_p^{mea}(t)$ and in myocardium tissue $C_T^{mea}(t)$ obtained from PET images can be described by

$$\begin{aligned} C_p^{mea}(t) &= C_p(t) + F_{mb} \times C_T(t) + e_1(t) \\ C_T^{mea}(t) &= C_T(t) + F_{bm} \times C_p(t) + e_2(t) \end{aligned} \tag{3}$$

where $C_p(t)$ and $C_T(t)$ are the true tracer concentrations in plasma and tissue; F_{mb} and F_{bm} represent the spillover constants from myocardium to blood and from blood to myocardium; and $e_1(t)$ and $e_2(t)$ are the measurement noise in plasma and tissue.

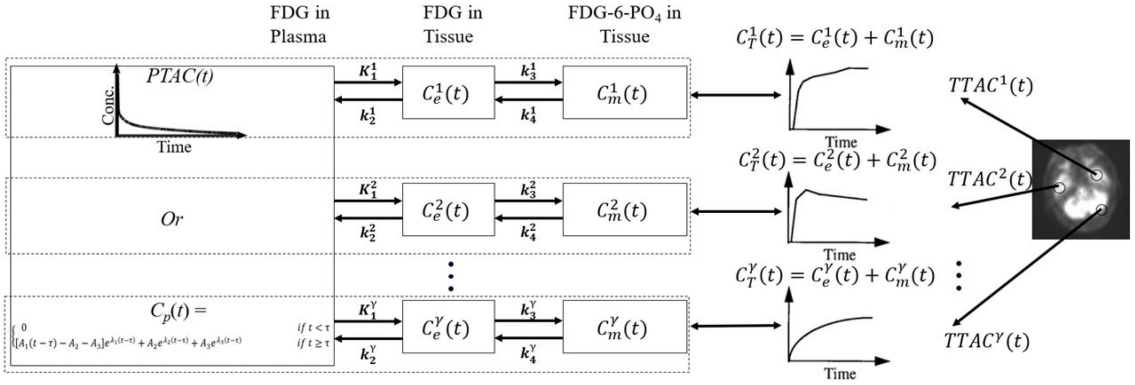

Fig. 3. Cascaded modeling approach for simultaneous estimation of PTAC and physiological parameters for FDG brain PET study, in which TTACs are the only measurements from the image(s).

A double (or a parallel) modeling approach was presented in [52], which was also referred to as a parallel simultaneous estimation, to estimate input/output functions ($C_p(t)$ and $C_T(t)$) and physiological parameters (K_1-k_4) simultaneously for dynamic cardiac studies. The PTAC model characterizing the tracer kinetics in plasma was used to account for the measurement noise, spillover of the input curve obtained from the left ventricular region on the PET images. Measured image-based LV PTAC and TTAC of the adjacent myocardial tissue were fitted simultaneously against both $C_p^{mea}(t)$ and $C_T^{mea}(t)$ simultaneously for the PTAC model and the FDG myocardial model with cross-contamination taken into account [52]. The simulation results demonstrated a more accurate estimate of the myocardial metabolic rate of glucose with improved reliability and provide an easier and more reliable alternative for partial volume and spillover corrections. This double modeling approach, which estimated the input and the output functions simultaneously, was generally applicable to a broad range of PET studies. To differentiate the following PTAC-based simultaneous estimation approaches, this approach can be referred to as the PTAC parallel modeling approach.

Please note that the approach described in Section IV-A requires the image-derived PTAC and TTAC measurements. The purpose of the parallel modeling approach is to estimate the "true" PTAC and TTAC "in parallel" from the noisy and spillover corrupted measurements and to estimate physiological parameters simultaneously with improved accuracy.

Different from the model-based method for PTAC to estimate full physiological parameters (K_1-k_4), an approach was validated in human studies in the quantification of myocardial blood flow using a myocardial perfusion tracer Flurpiridaz, which has high first-pass extraction fraction with a simple perfusion model [53]. As the extraction fraction of Flurpiridaz was linearly proportional to myocardial blood flow, the extraction fraction was estimated from the image-derived LV PTAC and TTACs within the first 90 s after tracer injection, with an iterative procedure to regressively estimate the true LV PTAC and true TTACs for three myocardial territories.

B. PTAC-Based Cascaded Modeling Approach—A Case Study for Brain Studies

In brain studies, blood vessels often cannot be identified or seen at all from the brain images alone. In this case, a cascaded modeling approach was presented in [54] for extracting input function and multiple physiological parameters simultaneously for the FDG brain PET study. Therefore, PTAC embedded in the brain images needed to be extracted from the brain TTAC images together with the physiological parameters. When the PTAC model-based input function $C_p(t)$ was used, the simultaneous estimation method can be illustrated as in Fig. 3 with one input function cascaded with γ FDG models, where $C_e(t)$ is free FDG in tissues, and $C_m(t)$ is FDG-6-phosphate in tissues.

As PTAC measurement is available neither from the brain image(s) nor from somewhere else, the estimation of all parameters, the FDG model rate constants K_1^j-k_4^j, $j = 1, 2, \ldots, \gamma$, and $C_p(\lambda_1, \lambda_2, \lambda_3, A_1, A_2, A_3)$, is purely based on the TTACs for the multiple ROIs defined on brain images.

The relationship between the output function and the input function for each FDG model is as shown in

$$C_T^j(t) = \mathrm{CBV}^j \cdot C_p(t) + \left(1 - \mathrm{CBV}^j\right)\left(C_e^j(t) + C_m^j(t)\right) \quad (4)$$

where $j = 1, 2, \ldots, \gamma$, CBV^j is the cerebral blood volume in ROI^j.

For joint curves fitting of the TTACs derived from γ ROIs, a joint cost function $\Phi(\theta)$ can be defined to combine the fitting of all TTACs in

$$\Phi(\theta) = \sum_{i=1}^{n}\sum_{j=1}^{\gamma} W_{i,j}\left\{C_T^j(t_i) - \mathrm{TTAC}^j(t_i)\right\}^2 \quad (5)$$

where $W_{i,j}$ is the weighting factor, n is the number of PET imaging frames, and γ is the number of ROIs defined. All parameters, including the parameters of the input function $(\lambda_1, \lambda_2, \lambda_3, A_1, A_2, A_3)$ in (2) and the rate constants of the FDG model for each ROI, can be estimated simultaneously by minimizing the cost function $\Phi(\theta)$.

Computer simulation demonstrated that the method was able to estimate all the required parameters simultaneously by using TTACs of two or more ROIs with distinct kinetics [54]. More reliable parameter estimation can be achieved when additional TTACs were used. In our investigation, three ROIs with distinct TTACs were suggested to be used in practice for achieving reliable estimation and reduced computational cost. This cascaded modeling approach is expected to be applicable to other parts of the human body, in particular, where a relatively large blood pool cannot be seen directly in the FOV

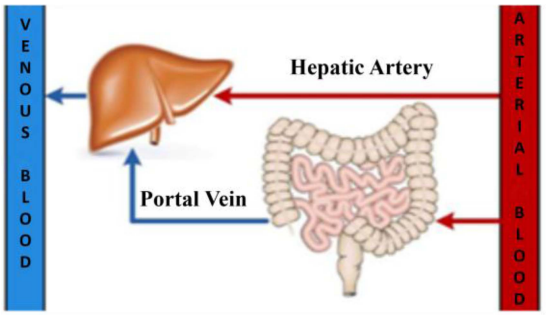

Fig. 4. Simple diagram showing the dual blood inputs to the liver.

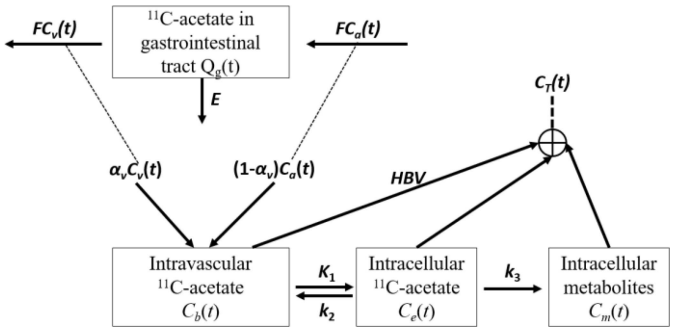

Fig. 5. ^{11}C-acetate liver kinetic model with dual inputs.

of the scanner. As TTAC is the output of a joint model with the PTAC model and the FDG model combined, this simultaneous estimation approach can be referred to as the PTAC model-based cascaded modeling approach.

The PTAC model-based simultaneous estimation (SIME) method was validated in human studies [55]. The results indicated that the input function can be accurately recovered from two or more ROIs in the human brain with distinct TTACs. No significant differences of CMRglu were found between the SIME method and the arterial input function. The SIME method was further applied to other tracers with various kinetic, e.g., it was validated in a myocardial perfusion study with SPECT tracer [56], and four PET tracers with 51 human subjects [57]. The SIME method was further extended by utilizing an input function derived from a simultaneously obtained DSC-MR scan [58].

Please note that the approach described in Section IV-B requires the image-derived TTACs from two or more ROIs where the tracer kinetics are distinct. There is no need to measure PTAC. Despite the increased computational complexity in parameter estimation as compared to the estimation for single ROI only, the cascaded modeling approach is capable of estimating the PTAC together with the physiological parameters, with a possibility of improved estimation accuracy of the physiological parameter, while PTAC cannot be identified/seen from the images under study.

C. PTAC-Based Dual-Input Function Modeling Approach—A Case Study for Liver Studies

The kinetic model in liver studies is different to a general kinetic model due to the liver has dual blood inputs, the hepatic artery (HA) and PV, as shown in Fig. 4. Thus, the dual blood inputs should be taken into account in kinetic modeling. A PTAC model-based dual-input modeling approach was proposed in [59] with ^{11}C-acetate to detect hepatocellular carcinoma (HCC).

Based on the conceptual diagram in Fig. 4, the kinetic model of ^{11}C-acetate can be described in Fig. 5. For the one-compartment gastrointestinal model at top left of Fig. 5, $C_a(t)$ is the PTAC in the HA and $C_v(t)$ is the blood from the PV. $C_v(t)$ can be regarded as the output of the one compartment model, while $C_a(t)$ is regarded as the input, and hence

$$C_v(t) = pe^{-(p+E)t} \otimes C_a(t), p = \frac{F}{\lambda V} \tag{6}$$

where F and E are parameters for the one-compartment gastrointestinal model, V is the gastrointestinal tissue, λ is the partition coefficient describing ratio of the solubility of ^{11}C-acetate in the gastrointestinal tissue and blood [59], and $\otimes$ is the convolution integration.

As shown in Fig. 5, the hepatic dual-input function should be taken into account for the liver kinetic model of ^{11}C-acetate. Hence, the dual-input function is a combination of $C_a(t)$ and $C_v(t)$ as shown in

$$\begin{aligned} C_b(t) &= (1-\alpha_v)C_a(t) + \alpha_v c_v(t) \\ &= (1-\alpha_v)C_a(t) + \alpha_v\left(pe^{-(p+E)t} \otimes C_a(t)\right) \end{aligned} \tag{7}$$

where $C_b(t)$ is ^{11}C-acetate concentration in the intravascular space or hepatic blood vessels, and α_v is the relative portal venous contribution to the hepatic blood flow.

The TTAC, $C_T(t)$, is a function of $C_b(t)$ as shown in

$$\begin{aligned} C_T(t) &= \text{HBV} \times C_b(t) + (C_e(t) + C_m(t)) \\ &= \text{HBV} \times C_b(t) + \left(B_1 + B_2 e^{-L_1 t}\right) \otimes C_b(t) \end{aligned} \tag{8}$$

where HBV is the hepatic blood volume constant, $C_e(t)$ and $C_m(t)$ are ^{11}C-acetate and metabolites concentrations in the intracellular space, respectively, and B_1, B_2, and L_1 are the parameters for the liver kinetic model of ^{11}C-acetate.

If $C_b(t)$ in (8) is replaced by (7), (8) will become a one-to-one function between $C_T(t)$ and $C_a(t)$, the PTAC from arterial, only. Thus, $C_T(t)$ will be expressed by $C_a(t)$, the PTAC of hepatic arterial, in

$$\begin{aligned} C_T(t) = \text{HBV} \times &\left((1-\alpha_v)C_a(t) + \alpha_v\left(pe^{-(p+E)t} \otimes C_a(t)\right)\right) \\ &+ \left(B_1 + B_2 e^{-L_1 t}\right) \\ &\otimes \left((1-\alpha_v)C_a(t) + \alpha_v\left(pe^{-(p+E)t} \otimes C_a(t)\right)\right) \end{aligned} \tag{9}$$

Thus, we only require the measurements of TTAC from the liver and the measurements of PTAC from a nearby arterial, to estimate all of the parameters in (9). In [59], arterial PTAC, $C_a(t)$, was measured from the ROI over the abdominal aorta. This approach can eliminate the measurement of PTAC in PV, which is difficult to be measured. In addition, the PTAC in PV can be estimated from this combined modeling process, through the dual-input functions of the one-compartment gastrointestinal model in Fig. 5.

The heterogeneous distribution and proportion of the two hepatic blood supplies were found in tumor and nontumor liver tissues [60]–[62]. To further improve the accuracy of the

proposed method, the individual proportion between HA and PV was included in parameter estimation. The parameter α_v, the ratio of the EIFs, was found to statistically improve the characterization of the ^{11}C-acetate kinetics. The analysis also provided a better understanding of the blood supply mechanism in the liver, which suggested the estimated α_v may provide an alternative diagnostic indicator of HCC.

Please note that the approach described in Section IV-C requires the image-derived PTAC (from arterial) and TTAC. The purpose of the dual-input modeling approach is to estimate additional input function from PV, which is very hard to measure, and to estimate additional parameters, such as α_v.

This PTAC model-based noninvasive simultaneous estimation approach described in Sections III and IV has several advantages.

1) The estimation of PTAC requires much less sampling points and alleviates the need for the measurement of the PTAC peak value, as both of the peak value and time can be obtained from the estimated PTAC. In addition, the estimated PTAC can greatly smooth the input function noise and improve the physiological parameter estimation accuracy (Section III).
2) It can incorporate simultaneous spillover, and potentially partial volume, correction and hence improve the parameter estimation accuracy (Section IV-A—parallel modeling approach).
3) It can simultaneously estimate PTAC itself and physiological parameters directly from the images, when the image-derived input function approach is not practical for conventional scanners (Section IV-B—cascaded modeling approach).
4) The indirectly estimated PTAC is likely to be the direct tracer TAC that drives the tracer TACs in adjacent tissue (TTACs) (Section IV-B—cascaded modeling approach).
5) The estimation of multiple input functions for organs such as the liver may result an alternative/additional diagnostic information, i.e., α_v, the relative portal venous contribution to the hepatic blood flow, which may provide an important, additional and alternative indicator for liver cancer detection (Section IV-C—dual-input function modeling approach).

Despite its success, SIME still has a lot of room to improve, such as its cost function convexity [6] and reducing its computational complexity.

V. Conclusion

This article provides a brief review of noninvasive input function acquisition and simultaneous estimations with physiological parameters for PET quantification for certain tracers. We first provide a brief survey of the two classes of the most commonly used approaches toward noninvasive input function acquisition, i.e., the population-based and image-derived methods for the measurement PTAC. This article also provides a brief survey of another class of noninvasive input function acquisition approach with an additional advantage of simultaneous estimations with physiological parameters for PET quantification, based on a generic analytical expression of the PTAC model. As the PTAC model-based simultaneous estimation approach is intended to improve the quality of quantification, it is expected that the image-derived PTAC from the total-body PET scanner together with the PTAC model-based simultaneous estimation approach will advance future PET absolute quantitative studies.

Acknowledgment

The authors would acknowledge Henry S. C. Huang for insightful discussions in this research area; Michael Fulham, Stefan Eberl, and Jinman Kim for helpful suggestions regarding the manuscript; and Tian Xia for professional technical support; as well as the support from Australia Research Council (ARC) grants for PET modeling and image processing theoretical research.

References

[1] M. E. Phelps, S. C. Huang, E. J. Hoffman, C. Selin, L. Sokoloff, and D. E. Kuhl, "Tomographic measurement of local cerebral glucose metabolic-rate in humans with (F-18)2-fluoro-2-deoxy-D-glucose—Validation of method," *Ann. Neurol.*, vol. 6, no. 5, pp. 371–388, 1979.
[2] M. Reivich *et al.*, "Fluorodeoxyglucose-F-18 method for the measurement of local cerebral glucose-utilization in man," *Circulation Res.*, vol. 44, no. 1, pp. 127–137, 1979.
[3] L. Sokoloff *et al.*, "Deoxyglucose-C-14 method for measurement of local cerebral glucose-utilization—Theory, procedure, and normal values in conscious and anesthetized albino-rat," *J. Neurochem.*, vol. 28, no. 5, pp. 897–916, 1977.
[4] K. Chen *et al.*, "Noninvasive quantification of the cerebral metabolic rate for glucose using positron emission tomography, F-18-fluoro-2-deoxyglucose, the Patlak method, and an image-derived input function," *J. Cerebral Blood Flow Metabolism*, vol. 18, no. 7, pp. 716–723, Jul. 1998.
[5] R. E. Carson and P. H. Kuo, "Brain-dedicated emission tomography systems: A perspective on requirements for clinical research and clinical needs in brain imaging," *IEEE Trans. Radiat. Plasma Med. Sci.*, vol. 3, no. 3, pp. 254–261, May 2019.
[6] J. D. Gallezot, Y. H. Lu, M. Naganawa, and R. E. Carson, "Parametric imaging with PET and SPECT," *IEEE Trans. Radiat. Plasma Med. Sci.*, vol. 4, no. 1, pp. 1–23, Jan. 2020.
[7] I. S. Yetik and J. Y. Qi, "Direct estimation of kinetic parameters from the sinogram with an unknown blood function," in *Proc. 3rd IEEE Int. Symp. Biomed. Imag. Macro Nano*, New York, NY, USA, 2006, pp. 295–298.
[8] A. J. Reader and H. Zaidi, "Advances in PET image reconstruction," *PET Clinics*, vol. 2, no. 2, pp. 173–190, 2007.
[9] E. V. R. Di Bella, R. Clackdoyle, and G. T. Gullberg, "Blind estimation of compartmental model parameters," *Phys. Med. Biol.*, vol. 44, no. 3, pp. 765–780, Mar. 1999.
[10] M. Bentourkia *et al.*, "A standardized blood sampling scheme in quantitative FDG-PET studies," *IEEE Trans. Med. Imag.*, vol. 18, no. 5, pp. 379–384, May 1999.
[11] A. Kato, D. Menon, M. Diksic, and Y. L. Yamamoto, "Influence of the input function on the calculation of the local cerebral metabolic-rate for glucose in the deoxyglucose method," *J. Cerebral Blood Flow Metabolism*, vol. 4, no. 1, pp. 41–46, 1984.
[12] S. Takikawa *et al.*, "Noninvasive quantitative fluorodeoxyglucose PET studies with an estimated input function derived from a population-based arterial blood curve," *Radiology*, vol. 188, no. 1, pp. 131–136, Jul. 1993.
[13] S. Eberl, A. R. Anayat, R. R. Fulton, P. K. Hooper, and M. J. Fulham, "Evaluation of two population-based input functions for quantitative neurological FDG PET studies," *Eur. J. Nucl. Med.*, vol. 24, no. 3, pp. 299–304, Mar. 1997.
[14] K. Wakita *et al.*, "Simplification for measuring input function of FDG PET: Investigation of 1-point blood sampling method," *J. Nucl. Med.*, vol. 41, no. 9, pp. 1484–1490, Sep. 2000.
[15] S. Takagi *et al.*, "Quantitative PET cerebral glucose metabolism estimates using a single non-arterialized venous-blood sample," *Ann. Nucl. Med.*, vol. 18, no. 4, pp. 297–302, Jun. 2004.
[16] G. J. R. Cook, M. A. Lodge, P. K. Marsden, A. Dynes, and I. Fogelman, "Non-invasive assessment of skeletal kinetics using fluorine-18 fluoride positron emission tomography: Evaluation of image and population-derived arterial input functions," *Eur. J. Nucl. Med.*, vol. 26, no. 11, pp. 1424–1429, Nov. 1999.
[17] T. Hirata *et al.*, "Reliability of one-point blood sampling method for calculating input function in (NaFPET)-F-18," *Nucl. Med. Commun.*, vol. 26, no. 6, pp. 519–525, Jun. 2005.

[18] P. Zanotti-Fregonara, R. Maroy, M. A. Peyronneau, R. Trebossen, and M. Bottlaender, "Minimally invasive input function for 2-F-18-fluoro-A-85380 brain PET studies," *Eur. J. Nucl. Med. Mol. Imag.*, vol. 39, no. 4, pp. 651–659, Apr. 2012.

[19] P. Zanotti-Fregonara *et al.*, "Population-based input function and image-derived input function for C-11 (R)-rolipram PET imaging: Methodology, validation and application to the study of major depressive disorder," *Neuroimage*, vol. 63, no. 3, pp. 1532–1541, Nov. 2012.

[20] S. S. Gambhir *et al.*, "Simple noninvasive quantification method for measuring myocardial glucose-utilization in humans employing positron emission tomography and F-18 deoxyglucose," *J. Nucl. Med.*, vol. 30, no. 3, pp. 359–366, Mar. 1989.

[21] I. N. Weinberg *et al.*, "Validation of PET-acquired input functions for cardiac studies," *J. Nucl. Med.*, vol. 29, no. 2, pp. 241–247, Feb. 1988.

[22] G. D. Hutchins, M. Schwaiger, K. C. Rosenspire, J. Krivokapich, H. Schelbert, and D. E. Kuhl, "Noninvasive quantification of regional blood-flow in the human heart using N-13 ammonia and dynamic positron emission tomographic imaging," *J. Amer. College Cardiol.*, vol. 15, no. 5, pp. 1032–1042, Apr. 1990.

[23] B. C. Chen *et al.*, "Noninvasive quantification of hepatic arterial blood-flow with nitrogen-13-ammonia and dynamic positron emission tomography," *J. Nucl. Med.*, vol. 32, no. 12, pp. 2199–2206, Dec. 1991.

[24] L. A. Green *et al.*, "Noninvasive methods for quantitating blood time-activity curves from mouse PET images obtained with fluorine-18-fluorodeoxyglucose," *J. Nucl. Med.*, vol. 39, no. 4, pp. 729–734, Apr. 1998.

[25] H. Iida *et al.*, "Noninvasive quantitation of cerebral blood flow using oxygen-15-water and a Dual-PET system," *J. Nucl. Med.*, vol. 39, no. 10, pp. 1789–1798, Oct. 1998.

[26] T. Ohtake *et al.*, "Noninvasive method to obtain input function for measuring tissue glucose-utilization of thoracic and abdominal organs," *J. Nucl. Med.*, vol. 32, no. 7, pp. 1432–1438, Jul. 1991.

[27] G. Germano, B. C. Chen, S. C. Huang, S. S. Gambhir, E. J. Hoffman, and M. E. Phelps, "Use of the abdominal-aorta for arterial input function determination in hepatic and renal PET studies," *J. Nucl. Med.*, vol. 33, no. 4, pp. 613–620, Apr. 1992.

[28] B. C. Chen *et al.*, "A new noninvasive quantification of renal blood-flow with N-13 ammonia, dynamic positron emission tomography, and a 2-compartment model," *J. Amer. Soc. Nephrol.*, vol. 3, no. 6, pp. 1295–1306, Dec. 1992.

[29] V. Dhawan *et al.*, "Quantitative brain FDG PET studies using dynamic aortic imaging," *Phys. Med. Biol.*, vol. 39, no. 9, pp. 1475–1487, Sep. 1994.

[30] K. Chen and S. C. Huang, "New estimation method that accounts for the PET accumulated counts of the blood-time activity curves in tracer kinetic modeling," *J. Nucl. Med.*, vol. 34, no. 5, p. 40, May 1993.

[31] S. Rajeswaran *et al.*, "2-D and 3-D imaging of small animals and the human radial artery with a high-resolution detector for PET," *IEEE Trans. Med. Imag.*, vol. 11, no. 3, pp. 386–391, Sep. 1992.

[32] M. M. Khalighi *et al.*, "Image-derived input function estimation on a TOF-enabled PET/MR for cerebral blood flow mapping," *J. Cerebral Blood Flow Metabolism*, vol. 38, no. 1, pp. 126–135, Jan. 2018.

[33] Y. Su *et al.*, "Noninvasive estimation of the arterial input function in positron emission tomography imaging of cerebral blood flow," *J. Cerebral Blood Flow Metabolism*, vol. 33, no. 1, pp. 115–121, Jan. 2013.

[34] L. M. Wahl, M. C. Asselin, and C. Nahmias, "Regions of interest in the venous sinuses as input functions for quantitative PET," *J. Nucl. Med.*, vol. 40, no. 10, pp. 1666–1675, Oct. 1999.

[35] M. C. Asselin, V. J. Cunningham, S. Amano, R. N. Gunn, and C. Nahmias, "Parametrically defined cerebral blood vessels as non-invasive blood input functions for brain PET studies," *Phys. Med. Biol.*, vol. 49, no. 6, pp. 1033–1054, Mar. 2004.

[36] J. E. M. Mourik, M. Lubberink, U. M. H. Klumpers, E. F. Comans, A. A. Lammertsma, and R. Boellaard, "Partial volume corrected image derived input functions for dynamic PET brain studies: Methodology and validation for C-11 flumazenil," *Neuroimage*, vol. 39, no. 3, pp. 1041–1050, Feb. 2008.

[37] S. Zhou, K. W. Chen, E. M. Reiman, D. M. La, and B. C. Shan, "A method for generating image-derived input function in quantitative F-18-FDG PET study based on the monotonicity of the input and output function curve," *Nucl. Med. Commun.*, vol. 33, no. 4, pp. 362–370, Apr. 2012.

[38] H. Watabe *et al.*, "Noninvasive estimation of the aorta input function for measurement of tumor blood flow with O-15 water," *IEEE Trans. Med. Imag.*, vol. 20, no. 3, pp. 164–174, Mar. 2001.

[39] X. Zheng, G. Tian, S. C. Huang, and D. Feng, "A hybrid clustering method for ROI delineation in small-animal dynamic PET images: Application to the automatic estimation of FDG input functions," *IEEE Trans. Inf. Technol. Biomed.*, vol. 15, no. 2, pp. 195–205, Mar. 2011.

[40] M. Liptrot *et al.*, "Cluster analysis in kinetic modelling of the brain: A noninvasive alternative to arterial sampling," *Neuroimage*, vol. 21, no. 2, pp. 483–493, Feb. 2004.

[41] J. S. Lee, K. H. Su, W. Y. Chang, and J. C. Chen, "Extraction of an input function from dynamic micro-PET images using wavelet packet based sub-band decomposition independent component analysis," *Neuroimage*, vol. 63, no. 3, pp. 1273–1284, Nov. 2012.

[42] K. Berradja and N. Boughanmi, "Assessment of brain glucose metabolism with input function determined from brain PET images by means of Bayesian ICA and MCMC methods," *Computerized Med. Imag. Graph.*, vol. 36, no. 8, pp. 620–626, Dec. 2012.

[43] R. Mabrouk, F. Dubeau, and L. Bentabet, "Dynamic cardiac PET imaging: Extraction of time-activity curves using ICA and a generalized Gaussian distribution model," *IEEE Trans. Biomed. Eng.*, vol. 60, no. 1, pp. 63–71, Jan. 2013.

[44] K. H. Su, L. C. Wu, R. S. Liu, S. J. Wang, and J. C. Chen, "Quantification method in F-18 fluorodeoxyglucose brain positron emission tomography using independent component analysis," *Nucl. Med. Commun.*, vol. 26, no. 11, pp. 995–1004, Nov. 2005.

[45] S. Surti, A. R. Pantel, and J. S. Karp, "Total body PET: Why, how, what for?" *IEEE Trans. Radiat. Plasma Med. Sci.*, vol. 4, no. 3, pp. 283–292, May 2020.

[46] X. Z. Zhang *et al.*, "Total-body dynamic reconstruction and parametric imaging on the uEXPLORER," *J. Nucl. Med.*, vol. 61, no. 2, pp. 285–291, Feb. 2020.

[47] D. Feng, S. C. Huang, and X. M. Wang, "Models for computer-simulation studies of input functions for tracer kinetic modeling with positron emission tomography," *Int. J. Bio Med. Comput.*, vol. 32, no. 2, pp. 95–110, Mar. 1993.

[48] D. Feng and X. Wang, "A computer-simulation study on the effects of input function measurement noise in tracer kinetic modeling with positron emission tomography (PET)," *Comput. Biol. Med.*, vol. 23, no. 1, pp. 57–68, Jan. 1993.

[49] D. Feng, X. Wang, and H. Yan, "A computer-simulation study on the input function sampling schedules in tracer kinetic modeling with positron emission tomography (PET)," *Comput. Methods Programs Biomed.*, vol. 45, no. 3, pp. 175–186, Nov. 1994.

[50] X. J. Li, D. G. Feng, and K. W. Chen, "Optimal image sampling schedule for both image-derived input and output functions in PET cardiac studies," *IEEE Trans. Med. Imag.*, vol. 19, no. 3, pp. 233–242, Mar. 2000.

[51] X. J. Li, D. Feng, and K. P. Wong, "A general algorithm for optimal sampling schedule design in nuclear medicine imaging," *Comput. Methods Programs Biomed.*, vol. 65, no. 1, pp. 45–59, Apr. 2001.

[52] D. Feng, X. Li, and S. Huang, "A new double modeling approach for dynamic cardiac PET studies using noise and spillover contaminated LV measurements," *IEEE Trans. Biomed. Eng.*, vol. 43, no. 3, pp. 319–327, Mar. 1996.

[53] R. R. S. Packard, S. C. Huang, M. Dahlbom, J. Czemin, and J. Maddahi, "Absolute quantitation of myocardial blood flow in human subjects with or without myocardial ischemia using dynamic flurpiridaz F 18 PET," *J. Nucl. Med.*, vol. 55, no. 9, pp. 1438–1444, Sep. 2014.

[54] D. Feng, K.-P. Wong, C.-M. Wu, and W.-C. Siu, "A technique for extracting physiological parameters and the required input function simultaneously from PET image measurements: Theory and simulation study," *IEEE Trans. Inf. Technol. Biomed.*, vol. 1, no. 4, pp. 243–254, Dec. 1997.

[55] K. P. Wong, D. Feng, S. R. Meikle, and M. J. Fulham, "Simultaneous estimation of physiological parameters and the input function—In vivo PET data," *IEEE Trans. Inf. Technol. Biomed.*, vol. 5, no. 1, pp. 67–76, Mar. 2001.

[56] K. P. Wong, S. R. Meikle, D. Feng, and M. J. Fulham, "Estimation of input function and kinetic parameters using simulated annealing: Application in a flow model," *IEEE Trans. Nucl. Sci.*, vol. 49, no. 3, pp. 707–713, Jun. 2002.

[57] R. T. Ogden, F. Zanderigo, S. Choy, J. J. Mann, and R. V. Parsey, "Simultaneous estimation of input functions: An empirical study," *J. Cerebral Blood Flow Metabolism*, vol. 30, no. 4, pp. 816–826, Apr. 2010.

[58] H. Sari *et al.*, "Incorporation of MRI-AIF information for improved kinetic modelling of dynamic PET data," *IEEE Trans. Nucl. Sci.*, vol. 62, no. 3, pp. 612–618, Jun. 2015.

[59] S. Chen and D. Feng, "Evaluation of hepatocellular carcinoma with dynamic C-11-acetate PET: A dual-modeling method," *IEEE Trans. Nucl. Sci.*, vol. 55, no. 3, pp. 999–1007, Jun. 2008.

[60] S. Chen and D. Feng, "Novel parameter estimation methods for C-11-acetate dual-input liver model with dynamic PET," *IEEE Trans. Biomed. Eng.*, vol. 53, no. 5, pp. 967–973, May 2006.

[61] S. Chen, C. Ho, and D. Feng, "Functional imaging techniques for the evaluation of hepatocellular carcinoma using dynamic C-11-Acetate PET imaging," *Current Med. Imag. Rev.*, vol. 2, no. 2, pp. 205–214, May 2006.

[62] H. C. Choi, S. R. Chen, D. Feng, and K. P. Wong, "Fast parametric imaging algorithm for dual-input biomedical system parameter estimation," *Comput. Methods Programs Biomed.*, vol. 81, no. 1, pp. 49–55, Jan. 2006.